Composite Structures 107 (2014) 103–111

Contents lists available at ScienceDirect

Composite Structures

journal homepage: www.elsevier.com/locate/compstruct

Bending deformation limits of corrugated unidirectionally reinforced composites

A. Schmitz *, P. Horst

Institute of Aircraft Design and Lightweight Structures, TU Braunschweig, Hermann-Blenk-Strasse 35, 38108 Braunschweig, Germany

ARTICLE INFO

Article history:
Available online 1 August 2013

Keywords:
Corrugated laminate
Morphing skin
Homogenisation
Delamination
Deformation limit

ABSTRACT

This paper concerns about deformation limits of circular corrugated unidirectional reinforced composites for bending dominated applications. Hence, a two-dimensional analytical stress function approach is used which takes through-thickness normal stresses into account. Hereby, the possible failure modes, namely fibre fracture and layer delamination, of unidirectional laminated circular corrugated sheets are predicted. Additionally, the accurate representative bending stiffness in corrugated-direction is extracted by using an energy approach. The influence of corrugation geometric parameters on deformation limits and stiffness is experimentally as well as theoretically investigated. For this reason, large curvature validation experiments of four different corrugation types are conducted by means of a specially constructed bending device. Finally, bending charts are provided facilitating the choice of an appropriate corrugation geometry during a preliminary design phase.

1. Introduction

Structural adaption to prevailing operating conditions has always been a topic in aerospace applications, see e.g. the review of morphing applications by Barbarino et al. [1]. Especially continuous contour-variable airfoil [2,3] and wing [4,5] morphing offers increase of aerodynamic performance and possibilities. Recent morphing structures particularly benefit from high-performance fibre-reinforced composites (e.g. [6]). Currently, most morphing structures can be divided into an underlying kinematic mechanism (acting as variable rib) and the skin providing a smooth surface and bearing aerodynamic loads. Obviously, morphing skin structures must simultaneously meet counteracting requirements: Compliant and highly deformable in morphing-direction while providing still enough stiffness to counteract aerodynamic loads. An overview of suggested morphing skins is given by Thill et al. [7]. It turns out that most structures try to meet these conflicting specifications by imposing an extreme anisotropy: Compliance in morphing-direction is balanced by increased transverse stiffness. Thus, for instance, cellular (zero-poisson's ratio) honeycombs seem superior candidates for one-dimensional in-plane (area increasing) morphing, see Olympio and Gandhi [8,9].

Corrugated composites also show this extreme anisotropy. Additionally, the deformation until rupture is increased with respect to the base-laminate for in-plane as well as for curvature-morphing. Hence, *corrugated composites* (CC) are regarded as particularly suitable for morphing applications, see e.g. Ursache et al. [10] for a poly-morphing (bending/twisting) winglet or Thill et al. [11] for a morphing trailing edge. The disadvantage of a non-smooth outer surface due to the inherent waviness of CC is counteracted by Yokozeki et al. [12] by means of one-sided rubber-filling.

Research on CC places emphasis on the determination of stiffness, both by modelling approaches (e.g. [13–15]) and experiments (e.g. [16,17]), yet. However, experimental estimations regarding flexural properties are rare so far as bearing conditions become complex for corrugated sheets. Trapezoidal CC have been investigated in bending by Dayyani et al. [16] (three-point bending) and Ghabezi and Golzar [17] (cantilever bending). In contrast to flat sheets, through-thickness normal stresses are generated for initially curved structures when loaded. As fibre-reinforced plastics exhibit low strength in thickness-direction, layer separation may occur. During experiments delamination failure has been observed at the highly curved regions of trapezoidal CC, see [16,18]. Available modelling approaches omit the existence of radial stresses except the two-dimensional finite element approach by Kress and Winkler [14]. Beside representative stiffness properties, appropriate estimation of deformation limits is crucial for morphing skins. So far, fibre fracture due to bending strain is accounted by Winkler and Kress [19]. Finally, large deformation fatigue investigations of CC are only conducted by Thill et al. [18], yet.

The intention of this paper is to present design considerations based on fast, analytical methods during a preliminary design phase. Hereby, circular CC intended for bending operations are focussed on. A possible application is the highly contour-variable

* Corresponding author. Tel.: +49 (0)531 391 9910.
E-mail address: a.schmitz@tu-bs.de (A. Schmitz).

0263-8223/$ - see front matter © 2013 Elsevier Ltd. All rights reserved.
http://dx.doi.org/10.1016/j.compstruct.2013.07.048

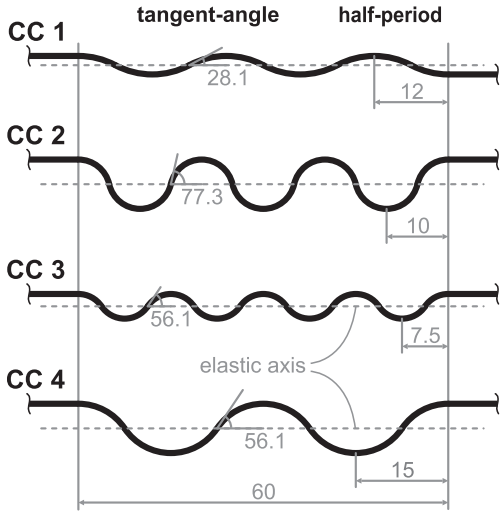

Fig. 1. Geometries of the four manufactured CC types (units are mm and deg).

droop nose presented by Burnazzi and Radespiel [20] from the aerodynamic point of view. In order to include delamination failure beside fibre fracture, the whole stress field in a two-dimensional corrugated cross-section is analysed. The structural curvature at rupture is predicted for unidirectional circular CC. Additionally, the bending stiffness in corrugated-direction is accurately modelled including through-thickness stresses. The applicability of the presented approaches is verified via bending experiments of four different corrugation types manufactured from carbon-fibre/epoxy composite. Precisely, the initial flexural modulus is determined by means of a three-point bending test and the structural curvature at rupture via a large-bending test. A specially constructed device subjects the samples to an almost pure state of bending. The fracture type (fibre fracture or delamination) is distinguished by visual inspection and sound emission. Finally, a bending chart of circular CC is provided to rapidly obtain an overview of appropriate corrugated geometries depending on operating requirements.

2. Materials and experiments

This section presents the constructed large bending setup, material data of carbon-fibre/epoxy and glass-fibre/epoxy base-material, the manufacturing and the geometry of the tested corrugated samples.

2.1. Manufacturing

Four differently corrugated sample types are manufactured, see Fig. 1. The geometry is assembled from circular segments and is completely described via the unit-cell's half-period c and the tangent-angle between adjacent circular segments Φ. All samples are manufactured from *unidirectional* (UD) carbon-fibre/HexPly913®-epoxy pre-impregnated layers with fibres aligned with the corrugation-direction. Four layers are individually hand-laid into a CNC-milled mould (Fig. 2) and cured at a temperature of 125 °C and 7 bar pressure to 1 mm nominal laminate thickness. Hereby, the use of counter-plates as illustrated in Fig. 2 gives considerably improved sample quality in terms of thickness variations compared to vacuum-bagging directly at the sample surface. Finally, the CC samples are cut to 23 mm width using a diamond saw.

In order to predict CC stiffness and deformation limits from base-material data, *flat plates* (FP) of the *carbon-fibre reinforced plastics* (CFRP) base-laminate are similarly processed and characterised, see Table 1. However, *glass-fibre reinforced plastics* (GFRP)

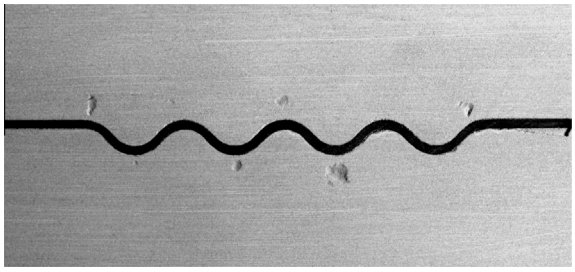

Fig. 2. CC 3 mould with counter-plate and inlaid sample.

is regarded as candidate morphing material [6]. Thus, material data of E-glass-fibre/HexPly®-epoxy composite are identified and given in Table 2. Herein, subscripts $\bullet_{\parallel}$ and $\bullet_{\perp}$ indicate fibre parallel and transverse properties, respectively. Further, $E^b_{\parallel}$ is the fibre parallel bending modulus obtained via three-point bending. Other data are in-plane tension (+) and compression (−) properties. However, bending, tension and compression tests require different sample thicknesses. Thus, along with the material data, the corresponding mean ply thickness t_{ply} is always given.

Finally, the precise ply thickness of the manufactured CC samples is measured via epoxy mounted and polished micrograph sections. All CC samples show resin accumulations (Fig. 3) at top and bottom of the circular segments. This effect is probably due to thermal expansions interacting with the inherently wavy geometry. Thus, the laminate thickness is measured at 70 equidistant locations along each sample type. At every point the total (t_{total}) and the fibre thickness without resin accumulation (t_{fibre}) are recorded. Both values, the resulting ply thickness and the geometry (tangent-angle and half-period) of the four CC types are summarised in Table 3. The resin accumulation fraction (t_{total}–t_{fibre}/t_{fibre}) ranges between 2.2% and 5.8%.

2.2. Large bending

In order to investigate deformation limits and corresponding fracture modes of CC under bending, large curvature bending

Table 1
Material data of HexPly913® CFRP (n = 5).

Prop.	CFRP	t^{FP}_{ply} (μm)
$E^b_{\parallel}$	89,819 MPa	272
$E^+_{\perp}$	9309 MPa	266
$E^-_{\perp}$	8499 MPa	260
$\nu_{\parallel\perp}$	0.304	266
$R^+_{\parallel}$	2176 MPa	266
$R^-_{\parallel}$	1040 MPa	260
$R^+_{\perp}$	43 MPa	266
$R^-_{\perp}$	182 MPa	260

Table 2
Material data of HexPly913® GFRP (n = 5).

Prop.	GFRP	t^{FP}_{ply} (μm)
$E^b_{\parallel}$	36,978 MPa	122
$E^+_{\perp}$	17,519 MPa	119
$E^-_{\perp}$	15,420 MPa	128
$\nu_{\parallel\perp}$	0.295	111
$R^+_{\parallel}$	1315 MPa	119
$R^-_{\parallel}$	1213 MPa	128
$R^+_{\perp}$	83 MPa	119
$R^-_{\perp}$	218 MPa	128